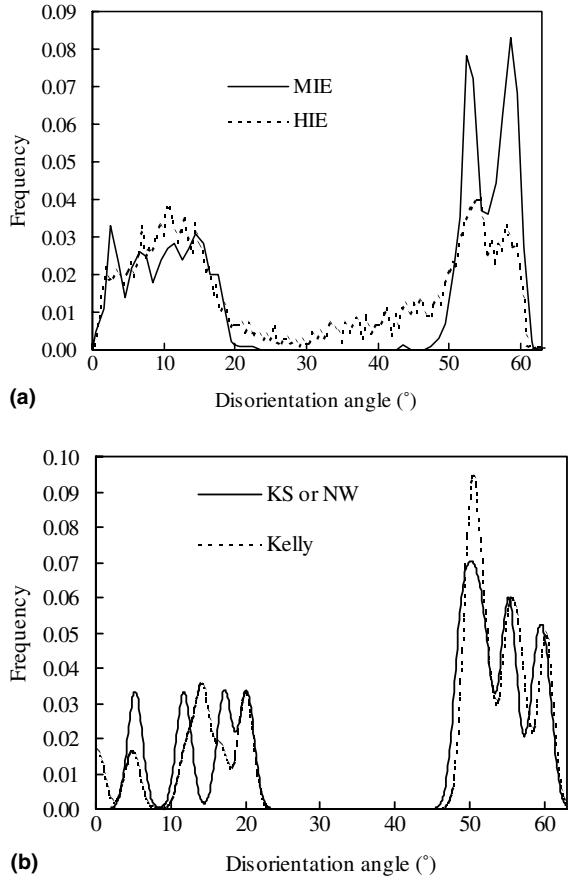

Fig. 6. Misorientation angle histogram between neighbouring bainite crystals within a single former austenite grain. (a) Experimental values. (b) Histogram computed assuming either (KS or NW) orientation relationships or 'Kelly' relationships (see Section 4.2) with austenite and no neighbourhood selection between bainite variants.

shows that low-angle boundaries are far more frequently observed than predicted by calculations. Moreover, the predicted peak around a misorientation angle of 20°, corresponding to variants in opposite locations in a given "Bain zone", was never observed experimentally. Thus, a "neighbourhood" or "local variant" selection seems to exist between bainite groups, and in particular there are "forbidden" pairs of neighbouring groups. This local variant selection has already been observed (although not always quoted) using EBSD or TEM with acicular ferrite [7], bainite [7,11,18,27] and martensite [7,12] microstructures.

3.4. Investigation of the bainite habit plane

Accurate determination of the habit plane of bainite laths is not possible, in particular in the HI microstructure, since interfaces between laths are not straight and thus not planar (Fig. 1). Here, the "habit" plane was defined as the straight, well-defined interfaces of bainite groups, which were readily observed in the partially transformed MI microstructures (Fig. 3(a)). A single-section trace analysis method was adopted to calculate "highly probable" indices for the habit plane. First, the crystallographic orientation of the former austenite grain was calculated from EBSD maps as explained before. Then, for each particular bainite group, the morphological and crystallographic orientations were measured and the crystallographic indices of the straight interface on the sample surface were then compared to the calculated traces of several $\{hkl\}_\gamma$ plane families. Following data on low-carbon lath martensite, and as the straight interfaces were parallel to the directions of the martensite laths in the partially transformed microstructures, three plane families were chosen, namely, $\{111\}_\gamma$, $\{223\}_\gamma$, and $\{557\}_\gamma$, as expressed in the $\langle 001\rangle_\gamma$ frame of the austenite phase. The results are given in Fig. 7. Obviously, a significant number of traces are far from any trace of $\{111\}_\gamma$ planes. In addition, more than four directions for the interface traces were observed within a single austenite grain, and the multiplicity of the $\{111\}_\gamma$ planes in face-centred cubic austenite is only four. Thus, the $\{111\}_\gamma$ family can be discarded. The habit plane of the low-carbon bainite investigated in this study thus differs from the $\{111\}_\gamma$ planes found in steels containing 0.2–0.78 wt% carbon [28–30]. Both $\{223\}_\gamma$ and $\{557\}_\gamma$ families satisfactorily match the experimentally observed traces. As matching appears to be slightly better for the $\{557\}_\gamma$ family, it was chosen as a "highly probable" habit plane family for the investigated bainite microstructure, consistently with results already obtained with low-carbon lath martensite [12,31–33] and bainite [34].

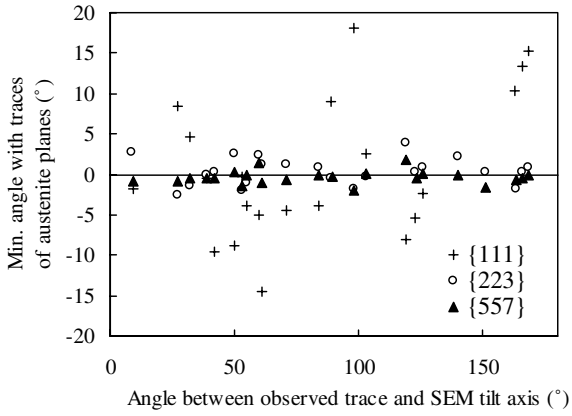

Fig. 7. Angle between the observed trace of the bainite habit plane and the closest trace of $\{111\}_\gamma$, $\{223\}_\gamma$ and $\{557\}_\gamma$ in the MI microstructure.

4. Discussion and modelling

4.1. Relationships between bainite packet properties and resistance to cleavage fracture

4.1.1. Bainite packet formation

To further investigate the formation of bainite packets, a number of partially formed bainite packets